

Contents lists available at [ScienceDirect](http://www.sciencedirect.com)

Journal of Aerosol Science

journal homepage: www.elsevier.com/locate/jaerosci

A simplified mathematical model for predicting cross contamination in displacement ventilation air-conditioned spaces



Carine Habchi, Kamel Ghali, Nesreen Ghaddar*

Mechanical Engineering Department, American University of Beirut, P.O. Box 11-0236, Beirut 1107-2020, Lebanon

ARTICLE INFO

Article history:

Received 5 March 2014

Received in revised form

3 May 2014

Accepted 19 May 2014

Available online 22 June 2014

Keywords:

Cross contamination

Displacement ventilation

Aerosols

Particle transport

ABSTRACT

The aim of this work is to develop a mathematical multi-plume multi-layer transport model of active particle behavior in spaces ventilated by a displacement ventilation (DV) system in order to study cross-infection between occupants in typical internal offices. The developed model incorporates particle deposition on walls and the effect of gravitational settling on particles distribution. The model was validated using published data from the literature revealing that the current simplified model is able to capture the physics of the problem and predict particle concentration and transport at low computational cost.

The model results show that as the particle diameter increases, the gravitational settling increases, thereby lowering the stratification in particle concentration created by the DV system and thus increasing the particle concentration at the breathing level of the exposed person. For a flow rate of 60 L/s, this effect remains until reaching a particle diameter above 10 μm where deposition on the floor opposing the DV principle acts as a removal factor. For the critical inhalable range, as the diameter increases, gravitational settling accumulates particles in the occupied zone, thereby increasing the probability of cross-infection. To overcome the settling effect, higher ventilation air flow rates are recommended to provide good indoor air quality (IAQ).

© 2014 Elsevier Ltd. All rights reserved.

1. Introduction

Exhaled droplets produced by the different human respiratory activities (breathing, coughing, and sneezing) constitute one of the main sources of infectious particles in indoor environments (Fanger et al., 1988). Human exhaled droplets are subject to fast evaporation before reaching their equilibrium diameter of droplets nuclei (Chen & Zhao, 2010; Morawska et al., 2009; Nicas et al., 2005). Droplets with equilibrium diameter smaller than 15 μm fall within the human inhalable range (Dockery & Pope III, 1994; Chen & Zhao, 2010; Nicas et al., 2005). In many cases, these emitted particles (droplets after evaporation) become airborne and can spread within the space before being escaped, deposited or inhaled by other healthy occupants (Lai & Cheng, 2007). The indoor particle dynamics depends largely on their diameter (size) and the air flow field associated with space air conditioning system. The heating, ventilation, and air conditioning (HVAC) system should be designed to effectively remove the contaminants as they are generated to minimize cross contamination between occupants.

* Corresponding author.

E-mail address: farah@aub.edu.lb (N. Ghaddar).

The displacement ventilation (DV) system is one of the ventilation systems that is known for its effectiveness in providing high indoor air quality at a lower energy cost and is widely used in office buildings (Bjørn & Nielsen, 2002; Price HVAC, 2014). Unlike conventional air conditioning systems, DV systems turn the air distribution system upside down by supplying fresh air near the floor level at a low velocity of less than 0.2 m/s and temperature greater than 18 °C to avoid thermal draft to occupants in the lower zone. The air motion of a DV system is mainly triggered by buoyancy forces creating the rising thermal plumes capable of carrying the contaminant away from the occupant's zone (Makhoul et al., 2013). This ventilation technique resulted in a thermal stratification leading to lower energy consumption compared to the conventional mixing ventilation system characterized by a homogeneous space temperature and indoor air quality (Etheridge & Sandberg, 1996; Brohus et al., 1996). The temperature stratification in DV system results in having two zones: a lower air temperature occupied zone and a higher air temperature zone (Makhoul et al., 2013). On the other hand, the contaminant floor-ceiling concentration profile depends largely on the relation between heat and contamination sources (Mundt, 1995). When heat sources are also the contamination sources, the rising convective thermal plumes (TP) emanating from the heat sources are expected to increase the ventilation effectiveness when using a displacement ventilation system (Brohus & Nielsen, 1996). In such a system, the air entrained by the convective thermal plumes will be warmed, transporting the contaminants upwards towards the ceiling where it is exhausted (Bjørn & Nielsen, 2002).

The effectiveness of the displacement ventilation in removing contaminants from the occupied zone has been extensively studied in the literature especially when it comes to tracer gas contaminants that can be easily picked up by the rising thermal plumes. For example, Mundt (1994) studied the effect of the DV system supply air flow rate, the heat source load and the room gradient temperature on the tracer gases spread within the space. Kanaan et al. (2010) developed a simplified model based on the Mundt (1994) model by combining all sources into a single source with the purpose of determining the clean zone bounded by the stratification height at which the plume upward flow is equal to supply air flow. Kanaan et al. (2010) determined carbon dioxide spread in spaces ventilated by chilled-ceiling displacement ventilation and decided on the optimized fraction of the return air in the DV supplied air that insures good indoor air quality in the occupied zone. However, the IAQ is not restricted to tracer gases such as CO₂ particles emanating from the occupants. If a clean occupied zone is desired, the particle concentration in the occupied zone should be determined for a wide range of particle diameters covering the inhalable range defined by particles of aerodynamic equivalent diameter lower than 15 μm (Miller et al., 1979). As the diameter of a particle increases, the gravitation effect increases acting against the upward air motion and thus challenging the performance of the DV system and complicating the modeling of the particle transport inside the space. In the above-mentioned literature models, the tracer gas contaminants are considered as passive particles characterized by a relatively low density and particle relaxation time and traveling at the same velocity of the flow field.

To our knowledge, simplified plume models simulating displacement ventilation and thermal plumes have not separated contaminant emitting and non-emitting contaminant sources or non-equal strength heat sources. Non-equal heat sources induce different critical plume heights that influence the presence of particles in the zone between stratification height and plumes critical heights (Kanaan et al., 2010). This is why most of the literature studies on active particle transport are conducted using computational fluid dynamics (CFD) models despite their costly computational time (Lai & Cheng, 2007; Gao et al., 2008; Li et al., 2011; Lai & Nielsen, 2011). Accurate prediction of particle deposition and transport using CFD for a flow field driven by buoyancy requires a fine mesh, resulting in a significant simulation time (Lai & Nielsen, 2011). Theoretical analysis relies on the understanding of the fundamental physics of the problem and on the proper choice of reasonable assumptions to simplify the complex problem. In addition simplified models that capture physics have a small computational overhead and still form a crucial part of the design process (Acred & Hunt, 2014). Therefore, it is very important to extend the simplified DV models that were developed for the passive contaminants to include non-equal sources with different critical heights as well as active particles that are largely present in indoor environments and account for induced particle transport by non-identical heat and particle generation sources. Modeling transport of active particles is more challenging due to the drift flux term resulting from the gravitational settling effect representing the relative velocity between the particle and the airflow (Zhao et al., 2009). Furthermore, deposition on surfaces is a physical process that affects particle concentration.

The aim of this work is to develop a simplified model that considers variable non-interacting heat plumes of different strength and particle generation rates to predict accurately the transport of active particles generated from an infected person in an indoor environment served by a DV air conditioning system at a significantly less computational time compared to CFD simulations. The model will consider both the effect of particle deposition on surfaces and gravitational settling on particle distribution within the space using the Lai & Nazaroff (2000) model for particle deposition on surfaces of different orientations taking into consideration gravitational effect and Brownian and turbulent diffusion. The model will be validated by comparison with published data on particle transport in DV-conditioned spaces. The validated simplified model will be applied to a typical internal office layout to investigate cross-contamination between two occupants. The study will determine the effect of particle size and DV supply air flow rate on active particle distribution and the ability of the DV system to ensure high indoor air quality while thermal comfort is sustained.

2. Description of the problem

The developed physical model will predict the temperature, velocity and concentration fields within a space ventilated by a DV system focusing on cross contamination between occupants, including particle deposition. Since the evaporation time for exhaled droplets within the inhalable equilibrium range is reported to be less than 1 s, it is very fast to affect the particle behavior (Morawska et al., 2009; Chen & Zhao, 2010; Nicas et al., 2005). Hence, for the inhalable range of interest in the current investigation, the evaporation process is neglected and droplets (after complete evaporation) are referred to as particles with equilibrium diameters that are less than 15 μm . To this end, the model will consider variable non-interacting heat plumes of different strengths representing the different internal sources encountered in office spaces (occupants, personal computers and office equipment). In addition, since internal sources of different geometries and heat strength are involved, the physical model should incorporate the expansion of the variable plumes at different critical heights to improve the prediction of particle concentration variation within the space which is largely affected by the rise and expansion of the buoyant thermal plumes.

Since displacement ventilation (DV) results in steady stratification in particle concentration and temperature fields in the vertical direction, the current DV+TP (combined displacement ventilation and thermal plumes) model for predicting the temperature and particle concentration field will be one dimensional. Accordingly, the space is divided into different vertical zones: lower (zone I), middle (zone II), and upper (zone III) as shown in Fig. 1a. Zone I is characterized by upward flow in the air surrounding the wall and thermal plumes. This zone extends from the floor to the stratification height, which is physically determined as the height for which the summation of the upward convective flows equals the supply flow rate. Zone II extends from the stratification height to the critical height of the strongest plume. Internal plumes of relatively weak strength will attain their critical height in this region and will merge with the surrounding air, while the strongest plume(s) will continue to rise in this zone to reach its (their) critical height and expand in zone III. Zone III is a recirculation zone where the circulating air and the last remaining rising plume(s) merge together.

As gradients in concentration, temperature, and velocity in the horizontal direction are small compared to vertical gradients of these variables, the domain is discretized vertically in several layers (Fig. 1a). At the horizontal level the layer is divided into lumped regions: internal source thermal plume regions, the wall plumes and the surrounding air regions constituting the air circulating between the plumes. In each lumped region the flow rates, temperature and concentration profiles will be determined according to empirical relations and energy and mass balances equations.

In order to predict the concentration field in the different vertical zones and lumped horizontal regions, the variable physical phenomena affecting particle distribution within the space will be included in the model. Figure 1b illustrates the different physics determining particles' behavior and the interaction between a rising thermal plume and the surrounding air due to lateral diffusion flux and room air entrainment by the thermal plume. Convection and diffusion are presented by

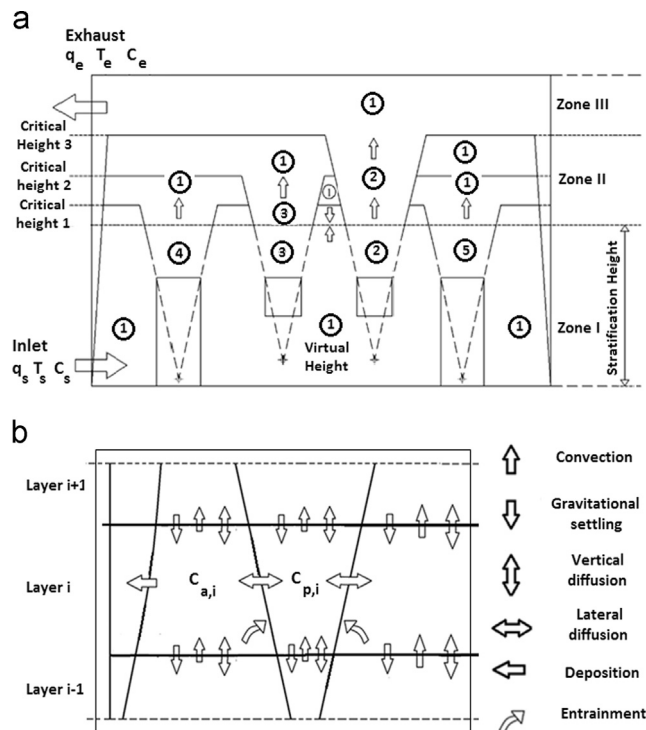


Fig. 1. Representation of (a) the discretized domain and (b) the physical phenomena affecting the contaminant concentration within a layer i .

the vertical convective and diffusive fluxes. In addition, since active particles are considered, gravitational effect and particle deposition on walls are included in the DV+TP model (see Fig. 1b).

3. Mathematical formulation

3.1. Plumes flow rates

In order to determine the particle distribution within the ventilated space, it is important to establish the flow field in the room. In DV systems, lateral air motion is neglected compared to vertical flow in the region below the recirculation zone. The resulting steady stratification height and the heights of the three zones are determined by the strength of the internal thermal plumes and the DV system air flow rate. The air flow rate of the rising plumes is adopted from the plume model of Mundt (1992) as follows:

$$M_{pl} = 2.38 \times 10^{-3} \rho Q_H^{3/4} \left(\frac{dT_\infty}{dz} \right)^{-5/8} m_n \quad (1a)$$

$$m_n = 0.004 + 0.039z_n + 0.38z_n^2 - 0.062z_n^3 \quad (1b)$$

$$z_n = 2.86 \times z_s \left(\frac{dT_\infty}{dz} \right)^{3/8} Q_H^{-1/4} \quad (1c)$$

where ρ is the air density, T_∞ the room temperature, z_s the point source height, Q_H is the heat source strength, and m_n and z_n the non-dimensional parameters. The mass flow rate entrained by the thermal plume $M_{ent,i}$ is given by

$$M_{ent,i} = M_{pl,i} - M_{pl,i-1} \quad (1d)$$

where $M_{pl,i-1}$ is the plume mass flow rate entering layer i and $M_{pl,i}$ is the plume mass flow rate exiting layer i .

Cylindrical heat sources are replaced by a virtual point source such that the border of the plume above the point source passes through the upper edge of the real cylindrical source (Goodfellow, 2001) with half-angle of the lateral spread of 12.5° (Rouse et al., 1952; Morton et al., 1956; Middleton, 1975). Hence, the plumes expansion geometry can be easily computed allowing the determination of the required minimum distance between any two internal heat sources to be considered non-interactive. The wall plume flow rate, M_w , at level z above the floor is determined by Jaluria (1980, chap. 4) expression

$$M_w = 2.87 \times 10^{-3} \rho (\Delta T_{wa})^{1/4} z^{3/4} X \quad (1e)$$

where X is the wall width and ΔT_{wa} is the difference in temperature between the wall and the surrounding air.

A mass balance for each horizontal layer gives the expression of the mass flow rate of the surrounding air $M_{a,i}$ as

$$M_{a,i} = M_s - \sum_{j=1}^n M_{w,(i,j)} - \sum_{k=1}^m M_{pl,(i,k)} \quad (1f)$$

where n refers to the vertical walls number within a layer i , and m to the number of remaining rising plumes, M_s is the mass supply flow rate, $M_{a,i}$, $M_{w,(i,j)}$, and $M_{pl,(i,k)}$, are, respectively, the mass flow rates of the surrounding air, the wall plumes and the internal thermal plumes at the interface between layers i and $i+1$.

The rising plume mathematical expressions of Mundt (1992) and Jaluria (1980, chap. 4) depend on the temperature field within the room which was determined using the thermal space model developed by Makhoul et al. (2012). The required input parameters for this model are the outdoor conditions, wall layering and properties and the strengths of the internal heat sources. Makhoul et al. (2012) took into consideration the different physical processes (such as convection, conduction, and so on) affecting the thermal field in order to determine the external and internal wall temperatures and the convective coefficients. The temperature variation within the space was determined by solving the energy balances for the different layers taking into consideration the different lumped regions within each layer. Hence, the vertical temperature gradient within the space is determined and then used in the calculation of the air, wall and plume flow rates within the different regions.

3.2. Modeling of particle distribution

The model should be able to capture the principal physics affecting particle behavior which, in addition to convection and deposition, include drag, gravitational settling, and turbulent and Brownian diffusion. Brownian and turbulent diffusion affect significantly particle behavior within the concentration boundary layer affecting particle deposition, and hence they are accounted for in the current model in addition to drag and gravitational settling effect. Other mechanisms that affect particle dispersion are Basset history, virtual mass, pressure gradient forces, thermophoresis, turbophoresis, electrophoresis, and virtual mass forces (Zhao et al., 2004, 2009). These mechanisms are reported to be one to several order of magnitudes smaller than the drag and gravitational forces and hence they are neglected in the current model (Zhao et al., 2004, 2009; Lai & Nazaroff, 2000; Zhao & Wu, 2006, 2007). Since temperature gradients in DV conditioned spaces are relatively small (less than 10°C), the thermophoresis can be neglected (Zhao & Wu, 2007).

In this study, steady particle generation by an infected person during normal respiratory activity will be investigated. Since exhaled velocities for breathing are relatively small, the exhaled jet will not disturb the rising thermal plume of the infected person (He et al., 2011). Therefore, the particle generation will be within the first layer of the thermal plume simulating the heat source-generating contaminant.

3.2.1. Particle distribution within the thermal plumes

The spread of particles within the space is largely dependent on the buoyant flows, gravitational effect and interaction between the surrounding air and the different internal plumes. To develop the particle conservation equation, the interactive diffusion between the thermal plume and its surrounding should be known. To this end, the parabolic particle profile developed by Kanaan et al. (2010) will be used in the current model:

$$c_{pl,i} = a_i + b_i \left(\frac{r}{R}\right)_i + c_i \left(\frac{r}{R}\right)_i^2 \quad (2a)$$

The constants a_i , b_i and c_i are determined for each layer i from the contaminant mass balances and concentration profile boundary conditions. At the thermal plume centerline the concentration gradient within each layer i is equal to zero ($b_i=0$) and at the boundary between the thermal plume and the surrounding air there is continuity of the contaminant concentration.

Once the concentration profile in the rising plumes is determined, the variation of particle concentration within each of the non-interactive internal thermal plumes should be determined as they interact with the surrounding air and affect the particle distribution within the space. What makes a contaminated plume different from a non-contaminated one is the generation term. The contaminant mass balance within any rising thermal plume numbered k is expressed by the following equation:

$$\begin{aligned} & [M_{pl,(i-1,k)}C_{pl,(i-1,k)} - M_{pl,(i,k)}C_{pl,(i,k)}] + [\rho v_s A_{pl,(i,k)}C_{pl,(i+1,k)} - \rho v_s A_{pl,(i-1,k)}C_{pl,(i,k)}] \\ & + \left[-A_{pl,(i-1,k)}D_p\rho \left(\frac{\partial C_{pl}}{\partial z}\right)_{i-1,k} + A_{pl,(i,k)}D_p\rho \left(\frac{\partial C_{pl}}{\partial z}\right)_{i,k} \right] \\ & + A_{int,(i,k)}(D_p + D_t)\rho \left(\frac{\partial C_{pl}}{\partial r}\right)_{R_i,z_{mi}} + M_{ent,(i,k)}C_{a,i} + S_{p,(i,k)} = 0 \end{aligned} \quad (2b)$$

The first term of Eq. (2b) represents the upward convective fluxes within the plume, the second term is the gravitational flux acting against the upward convective fluxes, the third term is the vertical diffusion flux, the fourth term illustrates the lateral diffusion interaction term, the fifth term is the entrainment flux and the last term the generation rate within the plume in layer i . The subscript i refers to the layer number, a to the air outside the thermal plumes (surrounding air), and pl to the air inside the thermal plume. The parameter $A_{pl,(i,k)}$ is the cross sectional area at the interface between the layers i and $i+1$ inside the thermal plume, $A_{int,(i,k)}$ is the interaction area between the plume k and its surrounding within layer i , C is the particle concentration, v_s the settling velocity, D_p the molecular diffusion coefficient, and D_t the turbulent diffusion coefficient. The source term $S_{p,(i,k)}$ accounts for particle generation within contaminated heat sources.

3.2.2. Particle distribution within the surrounding air

The contaminant mass balance in the room air surrounding the plumes is given by

$$\begin{aligned} & [\max(M_{a,i-1}; 0)C_{a,i-1} - (\max(M_{a,i}; 0) + \max(-M_{a,i-1}; 0))C_{a,i} + \max(-M_{a,i}; 0)C_{a,i+1}] \\ & + [\rho v_s A_{a,i}C_{a,i+1} - \rho v_s A_{a,i-1}C_{a,i}] + \left[A_{a,i}D_p\rho \left(\frac{\partial C_a}{\partial z}\right)_i - A_{a,i-1}D_p\rho \left(\frac{\partial C_a}{\partial z}\right)_{i-1} \right] \\ & - \sum_{k=1}^m A_{int,(i,k)}(D_p + D_t)\rho \left(\frac{\partial C_{pl,k}}{\partial r}\right)_{R_{(i,k)},z_{mi}} - \sum_{j=1}^n M_{ent,(i,k)}C_{a,i} - \sum_{j=1}^n \rho v_{d(i,j)}A_{w,(i,j)}C_{a,i} = 0 \end{aligned} \quad (2c)$$

The maximum function is introduced to account for the variation in the surrounding airflow direction allowing the equation to be applicable within the different zones defined in the vertical direction. For instance, the flow is upward below the stratification height while it is downward above the stratification height. In addition, due to the expansion of the internal plumes at different critical heights and their merging with the surrounding air region, the surrounding airflow may change in direction. The subscript j refers to the wall number within a layer surrounded by n walls, and k refers to the plume number of the m remaining rising plumes. The parameter $A_{a,i}$ represents the cross sectional area outside the thermal and wall plumes at the interface between the layers i and $i+1$ while $A_{w,(i,j)}$ represents the surface area of wall j within layer i .

The first term of Eq. (2c) represents the vertical convection flux of particles in the air surrounding the plumes, the second term is the gravitational flux, the third term is the vertical diffusion flux, the fourth term is the lateral particle diffusion fluxes presenting the interaction between the room air and the thermal plumes of the occupants due to concentration gradients, the fifth term represents the entrainment fluxes of surrounding air by the remaining rising plumes and the last one is the summation of deposition fluxes on walls within layer i . The deposition fluxes are determined as boundary conditions modeled by Lai & Nazaroff (2000).

3.3. Modeling of particle deposition

Deposition on surfaces is a determinant factor in the behavior of active particles and should be appropriately modeled. Boundary deposition fluxes J_d of particles towards the walls is determined from the expression of deposition velocities determined by Lai & Nazaroff (2000) as

$$J_d(y=0) = v_d C_\infty \quad (3)$$

where v_d is the deposition velocity on the corresponding wall, C_∞ is the core concentration outside the concentration boundary layer which in the current case is equal to the surrounding air concentration $C_{a,i}$ which vary with each layer, and y is the distance from the wall. Lai & Nazaroff (2000) determined the expression of deposition velocities including the Brownian and turbulent diffusion in addition to the gravitational settling effect on particle behavior for walls of different orientations. Their expressions have been adopted in the current model (Lai & Nazaroff, 2000) and we used an average friction velocity of 1.5 m/s which, within indoor environments, reported values between 0.3 and 3 cm/s. The sensitivity of the predicted particle concentration to friction velocity within the indoor range is verified by performing many simulations and the validity of this selected average value is verified when validating the model with published data from the literature.

4. Boundary conditions and numerical methods

The domain is discretized within the space into N layers in the vertical direction and a number of lumped regions in the horizontal direction depending on the number of non-interactive plumes of the internal sources. In order to run the algorithm solving for velocity, temperature and concentration fields in the studied room, the required inputs are the supply flow rate and temperature at the inlet, the indoor heat and contamination sources, and the outdoor conditions determining the imposed heat flux from the exterior. The space thermal model adopted from Makhoul et al. (2012) allowed the determination of wall temperatures but required the knowledge of indoor temperatures. On the other hand, the wall temperatures are required to solve for the energy balances of the different layers. For this reason, the solution for wall temperatures and indoor temperatures will be conducted by iteration connecting between the thermal space model and energy balances and at each step the mass flow rates which depend largely on the temperature gradients will be updated until convergence is reached as shown in the flowchart of Fig. 2. Once the flow rates are determined, they are used in solving the mass balances determining the concentration distribution within the space.

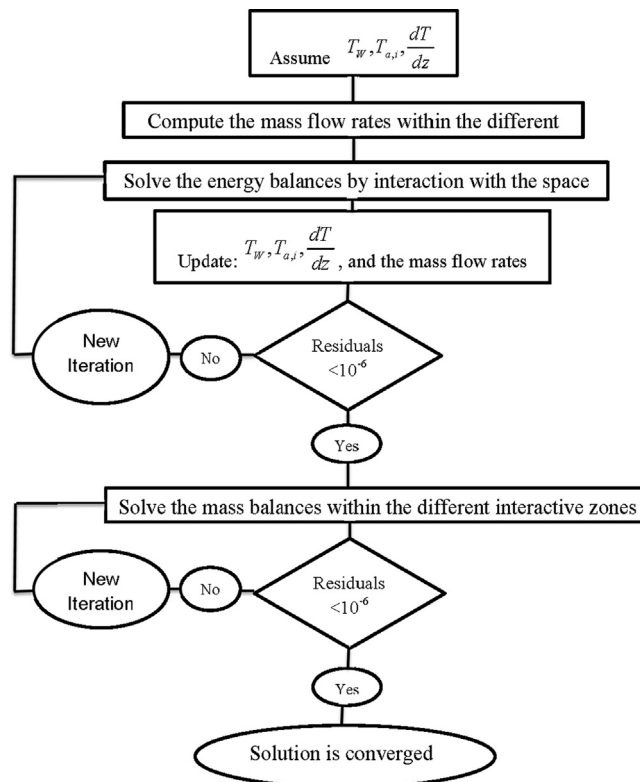


Fig. 2. Flowchart illustrating the sequence of operations for solving for the different variables.

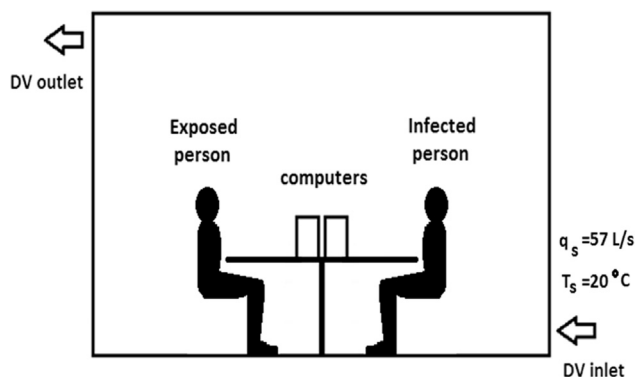


Fig. 3. Schematic of the set-up studied by Li et al. (2011) at the mid-plane.

The coupled mass and energy equations are discretized into algebraic equations using the finite volume method developed by Patankar (1980). The convergence criterion for the residuals of the different equations is set to 10^{-6} . The predicted variables are the concentrations within the internal plumes and surrounding air and temperature distribution in the room. In addition, the variation of friction velocity is found not to affect significantly the concentration of particles. For small particles less than $1 \mu\text{m}$, the variation in concentration due to change in friction velocity from 0.3 to 3 cm/s was in the order of 1% and for larger diameter particles concentration change was much less than 1%.

5. Results and discussions

5.1. Model validation

Extensive validation is performed in comparison with published data to insure that the current simplified model is capable of predicting cross-contamination within a space ventilated by a DV system. For the simplified plumes' model to be robust, it should predict deposition of particles on different surfaces accurately as well as the particle distribution within the different horizontal zones, particularly the air layer from which air is extracted to the breathing zone of the exposed person.

In order to validate the simplified model, the well-tested computational fluid dynamics (CFD) model developed by Li et al. (2011) was used. Their CFD model was validated by the experimental work of Lai et al. (2008) when studying steady-state particle distribution in a two-zone chamber. Their obtained results from the CFD model showed good agreement with experimental data insuring the accuracy of the CFD model in predicting the concentration and flow fields. Li et al. (2011) used their model to perform detailed CFD simulations to study particle behavior and cross-contamination between two occupants (60 W each): one representing the infected person and the other the exposed one in a typical office of dimensions $4 \text{ m} \times 3 \text{ m} \times 2.7 \text{ m}$. The space is ventilated by a DV system with air supply temperature of $20 \text{ }^\circ\text{C}$ and flow rate of 57 L/s (see Fig. 3). A 200 W flux from the window constitutes the external heat source. The concentration of generation was imposed as 0.05 g/m^3 for the different particle sizes of 1, 2.5, 5, and $10 \mu\text{m}$ at a breathing rate of 8.4 L/min.

The CFD case of Li et al. (2011) was simulated by the current model with the appropriate boundary conditions. The simplified model considered the case of three rising plumes and their expansion at different critical heights. Two rising plumes emanated from the infected and exposed persons while the two computers resulted in one rising plume. In the work of Li et al. (2011), the two computers (120 W each) were very close and their rising plumes can be lumped by an equivalent plume of double strength (Goodfellow, 2001). The averaged horizontal concentration (including the surrounding air and all the rising plumes) normalized by the concentration of generation was determined as a function of the height for different particle diameters. Furthermore, the intake fraction defined as the ratio of the concentration of particle at the breathing level of the exposed person to the concentration of generation was predicted for the variable diameters investigated. Total deposition rates (including deposition on surfaces other than walls) were also reported (Li et al., 2011).

Figure 4 shows the predicted variation of the average normalized concentration with height compared to published model results of Li et al. (2011) for different diameters of (a) $1 \mu\text{m}$; (b) $5 \mu\text{m}$; (c) $10 \mu\text{m}$. Although the simplified model predicted the concentrations within the different horizontal lumped regions, the variation of the average normalized concentration was found to be comparable with the results of Li et al. (2011) results. Good agreement is obtained between our model results and the published values of normalized concentrations with a maximum relative error of 5%, 8%, and 10%, respectively, for particles of 1, 5 and $10 \mu\text{m}$.

Since the breathing level of the target person is within the first layer of the non-infected plume, the concentration of particle within this zone was used to predict the intake fraction at the breathing level of the receiver. Figure 5 presents the intake fractions predicted by the current simplified model as well as the reported values by Li et al. (2011) for different particle sizes. The simplified model showed that the removal effectiveness is higher for fine particles, providing a relatively clean occupied zone and contaminated upper zone (Fig. 5). As the diameter increases, the gravitational effect becomes more pronounced, increasing particle concentration in the occupied region (Fig. 4) and hence increasing the intake fraction.

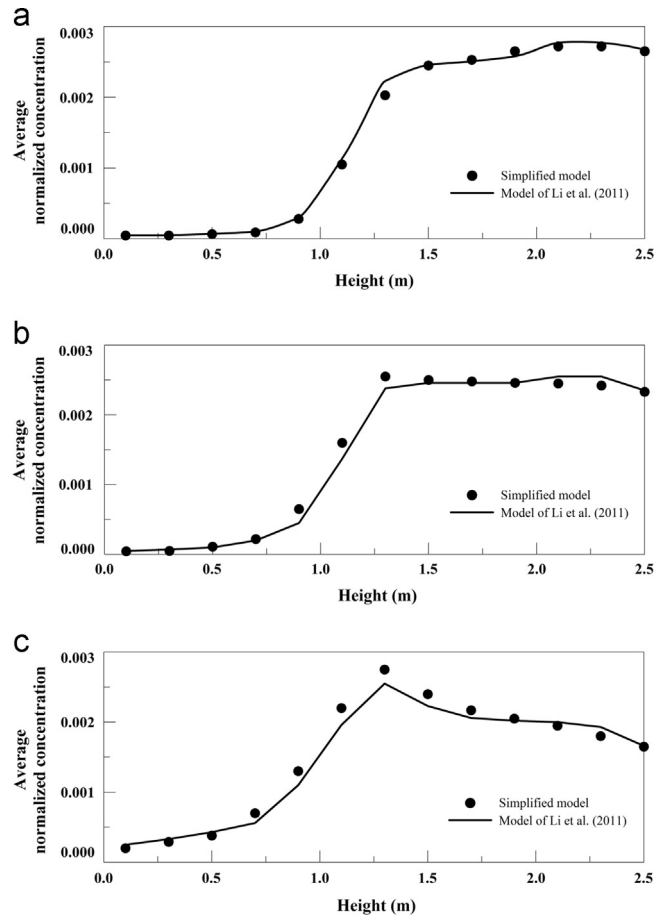


Fig. 4. Plot of the predicted variation of the average normalized concentration with height compared to the published model results of Li et al. (2011) at particle diameters of (a) 1 μm ; (b) 5 μm ; (c) 10 μm .

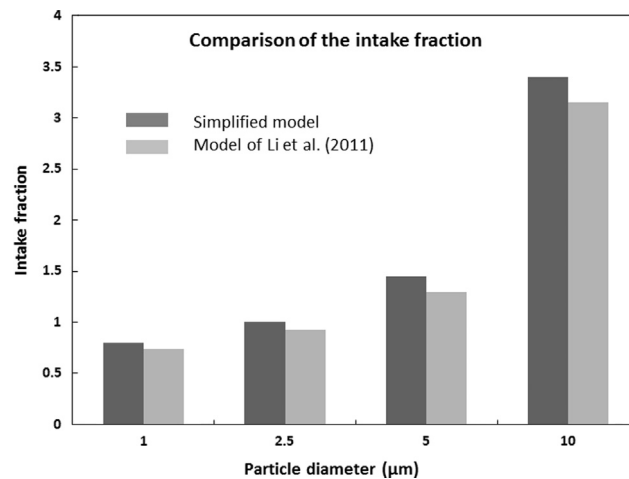


Fig. 5. Comparison of the intake fractions predicted for different diameters.

As shown in Figs. 4 and 5, the obtained results from our model and that of Li et al. (2011) match well with a relative error increasing from the fine to the coarse mode where it reaches 10%.

In the model of Li et al. (2011), deposition of particles was considered on different surfaces including occupants and desks. However, the simplified model accounts only for deposition on walls, neglecting deposition on other surfaces. This

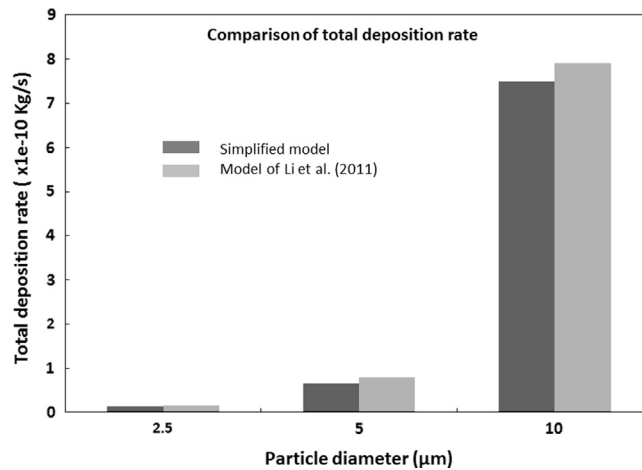


Fig. 6. Plot of the total rate of deposited mass of particles obtained from both our current model and that of Li et al. (2011) for different particle diameters (2.5, 5 and 10 µm).

assumption is validated by the comparison with the published model of Li et al. (2011). Figure 6 illustrates the total rate of deposited mass of particles obtained from both our current model and that of Li et al. (2011) for different particle diameters (2.5, 5 and 10 µm). It is expected that as the diameter increases, deposition on the desk, computers and humans increases due to the gravitational effect. This explains the increasing relative error in predicting total deposition with the increase in diameter. However, the relative errors observed are below 10% and hence the predicted results are within the engineering acceptable accuracy. In conclusion, the multi-plume simplified model in DV ventilated space is shown to accurately predict the average concentration, intake fraction and total deposition for the different particle sizes.

5.2. Case study

The developed model was applied to study the cross-contamination between occupants in typical offices ventilated by DV systems. For this goal, the simplified model was applied to a typical internal office layout occupied by an infected and an exposed person. The investigation of different supply conditions was performed to come up with recommendations on the required design of the DV system to satisfy both thermal comfort and IAQ criteria.

The domain consists of a room of dimensions (4 m × 3.5 m × 3 m), occupied by two sitting persons; one is generating particles representing the infected person and the other is the exposed person. The load distribution was selected to represent a typical internal office configuration: two sitting humans simulating two persons at rest (75 W each) equipped by their personal computer (100 W each), and lighting (50 W) constitute the internal heat sources, and a load of 150 W from the external wall is considered. For the studied case, four non-interactive thermal plumes (as in Fig. 1) are considered where the infected and exposed plumes of equal strength expand at the first critical height, and the two identical computer plumes expand at the second critical height because of their higher heat strength (in this case there is no additional distinct critical height). The inlet conditions of the supply airflow will be varied to satisfy the thermal and indoor air quality criteria. For instance, a low intake fraction is recommended at the breathing level of the exposed person for the inhalable range of particles, particularly for particle diameter lower than 10 µm constituting the critical range since they present the highest potential to penetrate the airways and reach the alveoli, thereby increasing the possibility of contaminating the exposed person (Mangili & Gendreau, 2005; Guha, 2008). In addition, the temperature in the occupied zone should be between 23 and 26 °C (BS EN ISO 7730: 1995) and the temperature difference between the feet and the head should not exceed 2 °C to 3 °C (BS EN ISO 7730: 1995). The supply temperature was fixed at 22 °C, which is 3 °C below the set-point room temperature to avoid thermal draught (Engineering Guide Displacement Ventilation). For this temperature, the flow rate will be changed until meeting all the load removal and IAQ requirements.

The flow rate largely affects the particles dispersion within the space and the level of the stratification height. For tracer gases, it is recommended to have the stratification height just above the breathing level to insure good IAQ (Brohus & Nielsen, 1996). Hence, the first flow rate investigated was 60 L/s insuring a level of 1.2 m for the stratification height that is slightly higher than the occupied zone which guarantees a high IAQ for tracer gases. The particle distribution was studied for different diameters within the inhalable range (0.1, 1, 2.5, 5, 7.5, 10, 12.5 and 15 µm). It was shown that for a flow rate of 60 L/s, the performance of the DV system in terms of IAQ for particle diameters between 5 and 12.5 µm is weakened due to the gravitational effect opposing the upward flow motion.

The particle diameter plays a major role in the determination of particle distribution within the space and deposition on different surfaces. Figure 7 shows the variation of the normalized particle concentration with height for different diameters (1, 5, 10, 12.5, 15 µm) from the fine to the coarse mode in the surrounding air zone for a flow rate of 60 L/s. Table 1 summarizes the predicted maximum normalized concentration and the normalized concentrations at the breathing level

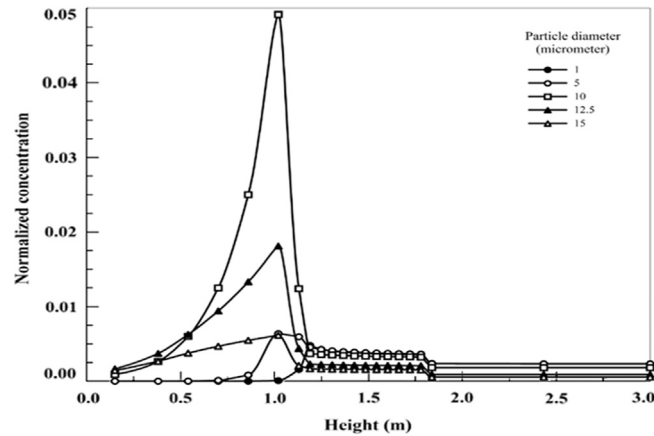


Fig. 7. Variation of the normalized particle concentration with height for different particle diameters in the surrounding air zone for a flow rate of 60 L/s.

Table 1

Influence of flow rate and particle diameter on normalized concentrations.

Stratification/critical 1 / critical 2 heights	Simulated case [q_s , d_p]	Normalized concentration (%) at the breathing level	Exhaust normalized concentration	Maximum normalized concentration in the surrounding air
1.2/1.75/1.85	[60,0.1]	1.4541e-4	2.333e-3	4.709e-3
	[60,1]	1.6542e-4	2.332e-3	4.788e-3
	[60,2.5]	2.6972e-4	2.329e-3	4.805e-3
	[60,5]	6.2965e-4	2.322e-3	6.379e-3
	[60,7.5]	1.202e-3	2.291e-3	2.728e-2
	[60,10]	1.31e-3	1.804e-3	4.915e-2
	[60,12.5]	4.687e-4	9.039e-4	1.811e-2
	[60,15]	2.2743e-4	5.456e-4	6.148e-3
1.3/1.9/2	[80,0.1]	5.213e-6	1.7497e-3	3.3354e-3
	[80,1]	5.461e-6	1.7496e-3	3.3365e-3
	[80,2.5]	8.433e-6	1.7484e-3	3.366e-3
	[80,5]	6.1402e-5	1.7436e-3	3.379e-3
	[80,7.5]	2.5702e-4	1.7342e-3	3.383e-3
	[80,10]	6.556e-4	1.7047e-3	5.668e-3
	[80,12.5]	9.477e-4	1.4396e-3	1.2116e-2
	[80,15]	5.398e-4	8.348e-4	8.253e-3
1.4/2.1/2.2	[100,0.1]	4.0062e-6	1.3998e-3	2.6854e-3
	[100,1]	4.0719e-6	1.3997e-3	2.6942e-3
	[100,2.5]	4.5157e-6	1.3987e-3	2.7072e-3
	[100,5]	1.0488e-5	1.3951e-3	2.7098e-3
	[100,7.5]	5.3548e-5	1.388e-3	2.7115e-3
	[100,10]	2.0382e-4	1.378e-3	2.7178e-3
	[100,12.5]	5.0561e-4	1.339e-3	3.2907e-3
	[100,15]	6.9509e-4	1.097e-3	6.074e-3

and at the exhaust for particles from 0.1 μm to 15 μm . As the particle diameter increases, the effect of the gravitational settling increases, resulting in: (1) a decrease in the exhaust concentration for all diameters, and (2) an increase in the maximum normalized concentration within the air for particle diameter below 10 μm (see Fig. 7). Furthermore, the maximum normalized concentration of the surrounding air (for particle diameters lower than 5 μm) occurs at the stratification level. For larger diameters the position of maximum concentration moves to levels below the stratification height of 1 m. The high concentration of particles below the stratification height is critical to the occupied zone since it is close to the breathing level and affects the quality of air drawn to the occupant breathing zone. Therefore, as the diameter of the particle increases, the DV system ability to maintain particle concentration stratification effect is lowered and thus the DV system's effectiveness is weakened in creating a lower clean occupied zone (Fig. 7) due to the downward gravitational settling effect that acts against the upward motion of the surrounding air below the stratification height. Therefore the protective effectiveness of the DV system relying on the transport of contamination within the rising contaminated plume to be exhausted at the ceiling level creating a relatively clean region within the occupied zone is reduced as the particle diameter increases.

Table 2
Influence of flow rate and particle diameter on particle deposition.

Simulated case [q_s , d_p] q_s (L/s): flow rate d_p (μm): particle diameter	% of particle deposition	Fraction of particles deposited on the vertical walls (%)	Fraction of particles deposited on the ceiling (%)	Fraction of particles deposited on the floor (%)
[60,0.1]	0.9	81.98	18.02	0
[60,1]	0.32	55.45	0	44.55
[60,2.5]	0.56	45.37	0	54.63
[60,5]	3.36	8.72	0	91.28
[60,7.5]	12.46	0.63	0	99.37
[60,10]	20.17	0.0225	0	99.9775
[60,12.5]	57.96	0.0038	0	99.9962
[60,15]	72.62	0.0015	0	99.9985
[80,0.1]	0.61	73.31	26.69	0
[80,1]	0.21	91.34	0	8.66
[80,2.5]	0.15	75.23	0	24.77
[80,5]	1.67	38.89	0	61.11
[80,7.5]	6.33	15.78	0	84.22
[80,10]	13.15	1.76	0	98.24
[80,12.5]	19.97	0.05	0	99.95
[80,15]	51.45	0.004	0	99.996
[100,0.1]	0.21	73.25	26.75	0
[100,1]	0.16	100	0	0
[100,2.5]	0.13	81.82	0	18.18
[100,5]	0.1	49.89	0	50.11
[100,7.5]	1.29	22.04	0	77.96
[100,10]	4.03	2.52	0	97.48
[100,12.5]	10.05	0.07	0	99.93
[100,15]	17.03	0.0075	0	99.9925

Table 2 illustrates the effect of flow rate and particle diameter on the percentage of deposition of particles and their distribution on different walls' orientation. For small diameters, turbulent diffusion and Brownian motion are the dominant physical mechanisms affecting deposition while gravitation plays a minor effect. This explains the high percentage of deposition on vertical walls and ceiling for sub-micrometer particles although the percentage of total deposition from those generated is relatively small. For large particle diameters, the effect of turbulent diffusion and Brownian motion on particle deposition is lower, leading to the decrease in percentage of particle deposition. On the other hand, the settling effect of larger particles is more pronounced. When the gravitational effect is significant, the percentage of deposition reaches relatively high values. For example for a flow rate of 60 L/s, total deposition is lower than 1% for particle diameters lower than 2.5 μm but increases significantly for larger/heavier particles reaching a value of 72.62% for particles of 15 μm with 99.99% depositing on the floor (see Table 2). Floor deposition plays a significant role in reducing particle exposure only for particle diameters larger than 10 μm . The deposition of particles on the floor acts against the principle of DV system featured with the reduction of contaminants in the occupied zone by entraining them into the upward buoyant flows. Deposition on the floor would not then play a positive role in particle removal unless it overcomes the upward flow in the surrounding air created by the DV system below the stratification height.

Figure 8 shows the predicted normalized particle concentration vertical distribution within the plumes of the computers and within the infected and the exposed person's plume zones and the surrounding air zone at a supply flow rate of 60 L/s and a particle diameter of 1 μm . As particles are generated within the thermal plume of the infected occupant, this plume favors their transport toward the ceiling level to be removed from the exhaust. This is why the highest concentrations of particles are within the plume zone of the infected person. As the plumes of the non-infected person and the computer one rise, they entrain relatively contaminated air from the surrounding. Therefore within the exposed person plume, the concentration increases gradually from the breathing level of the exposed person until the critical height of the plume, providing protection to a certain extent (see Fig. 8). As the surrounding zone constitutes the connection between the contaminated and exposed plumes, the concentration in this zone lies between the two. The merging of plumes within the surrounding at different critical heights is also illustrated in Fig. 8. At the level of the first critical height (approximately at 1.75 m), the plumes of the infected and exposed person merge with the surrounding. For the computer plumes, the plume expansion takes place at a higher level at the second critical height (approximately at 1.85 m).

The variation of the normalized concentration at the breathing level of the exposed person (Table 1) is determined by a balance between the upward flow motion of the DV system and the downward settling due to the gravitational effect on the particle. In the first stage, as the particle diameter increases the settling effect becomes stronger, which increases the concentration of particles in the occupied zone and thus augments the concentration at the breathing level of the exposed person, resulting in a decrease in the protection effectiveness provided by the ascending thermal plume of the exposed person. When the settling effect opposing the upward flow becomes dominant, the floor deposition increases significantly, thereby acting as a particle removal factor and thus decreasing the intake fraction as the particle diameter increases

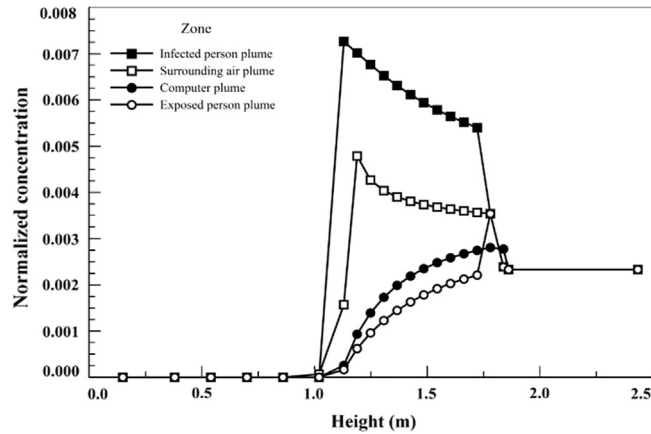


Fig. 8. Variation of the normalized particle concentration with height within the different zones for a flow rate of 60 L/s and a particle diameter of 1 micrometer.

(Tables 1 and 2). At a low flow rate of 60 L/s, it is observed that as the particle diameter increases from 0.1 μm to 10 μm , the particle normalized concentration at the breathing level of the exposed person is augmented, reaching a maximum value of 1.31×10^{-3} for 10 μm particles, which is relatively high. As the particle diameter exceeds 10 μm , the maximum normalized concentration decreases (see Fig. 8) due to settling and floor deposition, leading to a decrease in the particle normalized concentration at the breathing level of the exposed person (Table 1). The occurrence of the maximum intake fraction for a diameter of 10 μm within the critical range increases the risk of cross-infection between the occupants, which should be avoided. In other words, the gravitational effect associated with large particle sizes opposes the upward flow motion and results in accumulating particles below the stratification height, leading to a higher risk of cross-contamination unlike tracer gases (airborne particles). A higher level for the stratification height is required for large sized particles to satisfy the IAQ criteria for the inhalable range. This is achieved by increasing the flow rate to elevate the stratification height well above the breathing level of exposed occupants.

It is of interest to maintain the stratification effect for a wide range of particle diameters which can be achieved by increasing supply air flow rate to overcome the considerable downward settling motion for large diameter particles. This is demonstrated in Fig. 9 where the vertical variation of normalized concentrations within the surrounding air of different particle sizes is shown for higher DV supply flow rates of (a) 80 L/s and (b) 100 L/s. By increasing the supply flow rate from 60 to 80 L/s, the stratification and the first critical height are shifted upward respectively from 1.2 to 1.3 and from 1.75 to 1.9 m increasing the removal of contamination effectiveness leading to a considerable decrease of particles concentration in the space especially at the breathing level of the exposed person for a wide range of particle diameters. The effect of settling velocity is reduced as the upward flow velocities increase at higher flow rates. For example, the maximum intake fraction within the critical range decreased from 1.31×10^{-3} to 6.655×10^{-4} when the supply flow rate increased from 60 to 80 L/s (see Table 1). Additionally, the particle diameter at which the maximum intake fraction takes place is shifted from 10 to 12.5 μm , respectively (Table 1 and Figs. 7 and 9a), while the particle diameter above which the maximum normalized concentration takes place is shifted from 5 to 7.5 μm , respectively. At fixed particle diameter, the total deposition rate decreases as the flow rate increases due to the higher removal efficiency of the DV system. The particle diameter at which minimum deposition occurs is shifted from 1 to 2.5 μm due to the weakening of the gravitational settling effect. The IAQ performance at a DV flow rate of 80 L/s is much better than at 60 L/s. However, particles for diameters in the critical range between 7.5 and 10 μm still accumulate at the breathing level, thereby increasing the possibility of contamination. For this reason, when the flow rate was further increased to a value of 100 L/s, the maximum normalized concentration for particles less than 10 μm within the surrounding air takes place at the stratification level of 1.4 m approximately as seen in Fig. 9b. The maximum intake fraction within the critical range is decreased to 2.0832×10^{-4} (Table 1) for a flow rate of 100 L/s. Therefore, this flow rate is required to insure good IAQ criteria not only for tracer gases but also for particle diameters within the critical range. It can then be concluded that having a stratification height just above the breathing level (Brohus & Nielsen, 1996) is not enough for insuring good IAQ for the critical inhalable range, which is satisfied in our case study at a stratification height higher than 1.4 m.

As mentioned earlier, the supply air conditions should meet not only the IAQ criteria but also the thermal comfort and load removal requirements in the space. Therefore, the performance of the DV system in terms of thermal comfort for the different supply conditions studied was investigated and the results obtained are summarized in Table 3. As the flow rate varies from 60 to 100 L/s, the temperature difference between the feet and the head for a seated person decreases from 4.45 to 2.65 $^{\circ}\text{C}$ and the temperature range within the occupied zone is reduced from [23.33 $^{\circ}\text{C}$; 27.78 $^{\circ}\text{C}$] to [23.2 $^{\circ}\text{C}$; 25.85 $^{\circ}\text{C}$]. Thus as the flow rate increases from 60 to 80 L/s to 100 L/s, the performance of the DV system in terms of thermal comfort is enhanced. The two criteria for thermal comfort are both satisfied for the supply conditions of 22 $^{\circ}\text{C}$ and 100 L/s for which

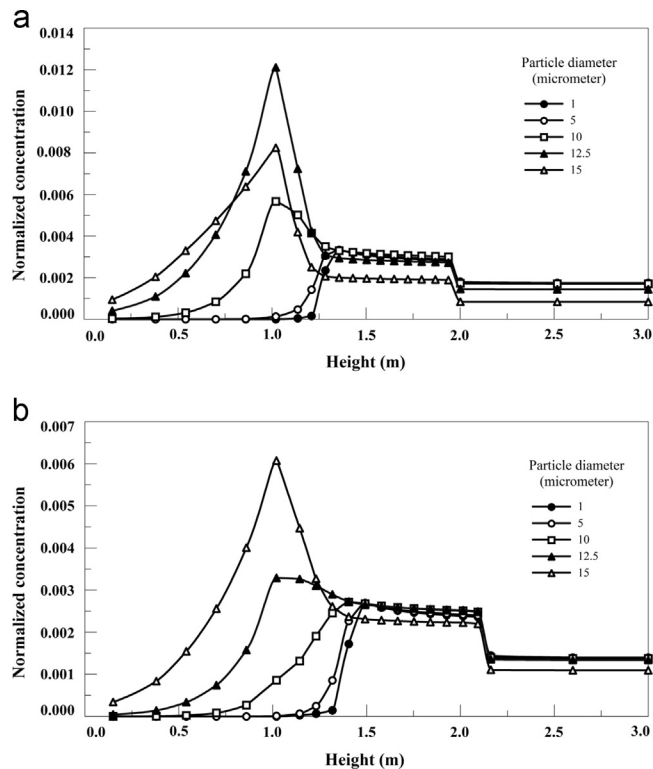


Fig. 9. Increase of the flow rate to meet the IAQ criteria to a value of: (a) 80 L/s; (b) 100 L/s.

Table 3

Performance of the DV system in terms of thermal comfort for different supply conditions.

Supply conditions [q_s , T_s] q_s (L/s): supply flow rate T_s (°C): supply temperature	Difference in temperature (°C) between the feet and the head	Temperature range in the occupied zone
[60,22]	4.45	[23.33; 27.78]
[80,22]	3.33	[23.24;26.57]
[100,22]	2.65	[23.2; 25.85]

the temperature in the occupied is between 23 and 26 °C (BS EN ISO 7730: 1995) and the temperature difference between the feet and the head is lower than 3 °C (BS EN ISO 7730: 1995).

6. Conclusion

A simplified model predicting active particle behavior in spaces ventilated by DV systems was developed. The developed model incorporated particles' deposition on walls of different orientations, and the gravitational settling affecting the particles' distribution within the space. Given that indoor heat sources have different heat loads, the expansion of rising plumes at different critical heights was considered in the new multi-plume model. The model ability in predicting particle concentrations, intake fractions and deposition rates for different particle diameters was validated using data from literature revealing that the current simplified model is capable of capturing the physics of the problem with significant reduction of the computational time cost. The validated model was used to study cross-infection between occupants in typical internal offices. Investigation of different supply conditions was performed to come up with recommendations on the required design of the DV system to satisfy both thermal comfort and IAQ criteria for the inhalable range particularly for a particle of diameter lower than 10 μm presenting high probability of infecting the exposed person if inhaled.

The model results showed that as the particle diameter increases from the sub-micrometer mode the effect of gravitational settling increases, lowering the stratification in concentration created by the DV system and thus increasing the particle concentration at the breathing level of the exposed person. For a flow rate of 60 L/s, this effect remains until reaching a particle diameter above 10 μm where deposition on the floor opposing the DV principle acts as a removal factor. For the critical inhalable range of interest, gravitational settling accumulates particles in the occupied zone as the diameter increases, leading to a higher probability of cross-infection. In general, a stratification height significantly above the breathing level ensures good IAQ for the critical inhalable range.

The developed model presents a computationally low-cost design tool that can be easily used in offices conditioned by DV system to ensure relatively safe intake fractions for the inhalable range and satisfy the thermal comfort criteria.

Acknowledgment

The authors would like to thank the Lebanese National Council for Scientific Research (CNRS) for their financial support. The support of the University Research Board (URB) at the American University of Beirut is also acknowledged as well as the Shammas Ph.D. Fellowship.

References

- Acred, A., & Hunt, G.R. (2014). A simplified mathematical approach for modelling stack ventilation in multi-compartment buildings. *Building and Environment*, 71, 121–130.
- Bjorn, E., & Nielsen, P.V. (2002). Dispersal of exhaled air and personal exposure in displacement ventilated rooms. *Indoor Air*, 12, 147–164.
- Brohus, H., Knudsen, H.N., Nielsen, P.V., Clausen, G., & Fanger, P.O. (1996). Perceived air quality in a displacement ventilated room. In: *Proceedings of the Indoor Air, 7th International Conference on Indoor Air Quality and Climate*, vol. 1, pp. 811–816.
- Brohus, H., & Nielsen, P.V. (1996). Personal exposure in displacement ventilated rooms. *Indoor Air*, 6, 157–167.
- B.S. EN ISO 7730 (1995). *Moderate Thermal Environments – Determination of the PMV and PPD Indices and Specification of the Conditions for Thermal Comfort*. British Standards Institute: London.
- Chen, C., & Zhao, B. (2010). Some questions on dispersion of human exhaled droplets in ventilation room: answers from numerical investigation. *Indoor Air*, 20(2), 95–111.
- Dockery, D.W., & Pope, C.A., III (1994). Acute respiratory effects of particulate air pollution. *Annual Review of Public Health*, 15, 107–132.
- Etheridge, D.W., & Sandberg, M. (1996). *Building Ventilation: Theory and Measurement*. Wiley: Chichester.
- Fanger, P.O., Lauridsen, J., Bluysen, P., & Clausen, G. (1988). Air pollution sources in offices and assembly halls, quantified by the olf unit, laboratory of heating and air conditioning, technical university of Denmark, DK-2800 Lyngby (Denmark). *Energy and Buildings*, 12, 7–19.
- Gao, N., Niu, J., & Morawska, L. (2008). Distribution of respiratory droplets in enclosed environments under different air distribution methods. *Building Simulation*, 1, 326–335.
- Goodfellow, H.D. (2001). *Industrial Ventilation Design Guidebook*. Academic Press: San Diego.
- Guha, A. (2008). Transport and deposition of particles in turbulent and laminar flow. *Annual Review of Fluid Mechanics*, 40, 311–341.
- He, Q., Niu, J., Gao, N., Zhu, T., & Wu, J. (2011). CFD study of exhaled droplet transmission between occupants under different ventilation strategies in a typical office room. *Building and Environment*, 46, 397–408.
- Jaluria, Y. (1980). *Natural Convection, Heat and Mass Transfer, Free Boundary Flows*. Pergamon Press: New York.
- Kanaan, M., Ghaddar, N., & Ghali, K. (2010). Simplified model of contaminant dispersion in rooms conditioned by chilled-ceiling displacement ventilation system. *HVAC&R Research*, 16, 765–783.
- Lai, A.C.K., & Cheng, Y.C. (2007). Study of expiratory droplet dispersion and transport using a new Eulerian modeling approach. *Atmospheric Environment*, 41, 7473–7484.
- Lai, A.C.K., & Nazaroff, W.W. (2000). Modeling indoor particle deposition from turbulent flow onto smooth surfaces. *Journal of Aerosol Science*, 31, 463–476.
- Lai, A.C.K., Wang, K., & Chen, F.Z. (2008). Experimental and numerical study on particle distribution in a two-zone chamber. *Atmospheric Environment*, 42, 1717–1726.
- Li, X., Niu, J., & Gao, N. (2011). Spatial distribution of human respiratory droplet residuals and exposure risk for the co-occupant under different ventilation methods. *HVAC&R Research*, 17, 432–445.
- Li, Y., & Nielsen, P.V. (2011). Commemorating 20 years of indoor air CFD and ventilation research. *Indoor Air*, 21, 442–453.
- Makhoul, A., Ghali, K., & Ghaddar, N. (2012). A simplified combined displacement and personalized ventilation model. *HVAC&R Research*, 18, 737–749.
- Makhoul, A., Ghali, K., & Ghaddar, N. (2013). The energy saving potential and the associated thermal comfort of displacement ventilation systems assisted by personalized ventilation. *Indoor Built Environment*, 22, 508–519.
- Mangili, A., & Gendreau, M.A. (2005). Transmission of infectious diseases during commercial air travel. *Lancet*, 365, 989–996.
- Morawska, L., Johnson, G.R., Ristovski, Z.D., Hargreaves, M., Mengersen, K., Corbett, S., Chao, C.Y.H., Li, Y., & Katoshevski, D. (2009). Size distribution and sites of origin of droplets expelled from the human respiratory tract during expiratory activities. *Journal of Aerosol Science*, 40, 256–269.
- Middleton, J.H. (1975). The asymptotic behavior of a starting plume. *Journal of Fluid Mechanics*, 72, 753–771.
- Miller, F.J., Gardner, D.E., Graham, J.A., Lee, R.E., Wilson, W.E., & Bachmann, J.D. (1979). Size considerations for establishing a standard for inhalable particles. *Journal of the Air Pollution Control Association*, 29, 610–615.
- Morton, B.R., Taylor, G., & Turner, J.S. (1956). Turbulent gravitational convection from maintained and instantaneous sources. *Proceedings of the Royal Society*, 234, 1–23.
- Mundt, E. (1992). Convection flows in rooms with temperature gradients – theory and measurements. In: *Proceedings of Roomvent Third International Conference on Air Distribution in Rooms*.
- Mundt, E. (1994). Contaminant distribution in displacement ventilation–Influence of disturbances. *Building and Environment*, 29, 311–317.
- Mundt, E. (1995). Displacement ventilation systems – convection flows and temperature gradients. *Building and Environment*, 30, 129–133.
- Nicas, M., Nazaroff, W.W., & Hubbard, A. (2005). Toward understanding the risk of secondary airborne infection: emission of respirable pathogens. *Journal of Occupational Environmental Hygiene*, 2, 143–154.
- Patankar, S.V. (1980). *Numerical heat transfer and fluid flow. Series in Computational Methods in Mechanics and Thermal Sciences*. Hemisphere Publishing Corporation: New York.
- Price HVAC. *Engineering Guide Displacement Ventilation*. (<http://www.pricevac.com/Catalog/Section/>) (accessed 01.02.2014).
- Rouse, H., Yih, C.S., & Humphreys, W. (1952). Gravitational convection from a boundary source. *Tellus*, 4, 201–210.
- Zhao, B., Chen, C., & Tan, Z.C. (2009). Modeling of ultrafine particle dispersion in indoor environments with an improved drift flux model. *Journal of Aerosol Science*, 40, 29–43.
- Zhao, B., & Wu, J. (2006). Modeling particle deposition from fully developed turbulent flow in ventilation duct. *Atmospheric Environment*, 40, 457–466.
- Zhao, B., & Wu, J. (2007). Particle deposition in indoor environments: analysis of influencing factors. *Journal of Hazardous Materials*, 147, 439–448.
- Zhao, B., Zhang, Y., Li, X., Yang, X., & Huang, D. (2004). Comparison of indoor aerosol particle concentration and deposition in different ventilated rooms by numerical method. *Building and Environment*, 39, 1–8.